Effect of material properties on integration damage in organosilicate glass films

E. Todd Ryan[a)] and Jeremy Martin
Advanced Micro Devices, AMD/Motorola Alliance, 3501 Ed Bluestein Boulevard, Austin, Texas 78721

Kurt Junker
Motorola, APRDL, 3501 Ed Bluestein Boulevard, Austin, Texas 78721

Jeff Wetzel
International SEMATECH, 2706 Montopolis Drive, Austin, Texas 78757

David W. Gidley and Jianing Sun
Department of Physics, University of Michigan, Ann Arbor, Michigan 48109

Most organosilicate glass[1] (OSG), low dielectric constant (low-κ) films contain Si–R groups, where R is an organic moiety such as $-CH_3$. The organic component is susceptible to the chemically reactive plasmas used to deposit cap layers, etch patterns, and ash photoresist. This study compares a spin-on, mesoporous OSG film with a completely connected pore structure to both its nonmesoporous counterpart and to another low-density OSG film deposited by plasma-enhanced chemical vapor deposition. The results show that the film with connected pores was much more susceptible to integration damage than were the nonmesoporous OSG films.

As integrated circuit device and interconnect dimensions continue to scale smaller, low dielectric constant (κ) interlayer dielectric (ILD) materials will become necessary to mitigate RC (product of resistance and capacitance) propagation delay and reduce power consumption and crosstalk.[1] Lowering the κ-value of a material requires either altering the chemical bonding to reduce the bond polarizability or decreasing the number of bonds (density) in a material.[2] To reduce the κ-value below 2.2, most dielectric materials will require a density decrease by introducing free volume (micropores < 2 nm in diameter) or mesoporosity (2–50 nm diameter pores). Unfortunately, lowering the density also compromises the mechanical strength and other properties of the material.[2]

The material properties of mesoporous dielectric films, such as connected pores and low mechanical strength, create a host of integration problems including integration damage to the film.[3,4] The Si–R groups make organosilicate glass (OSG) films hydrophobic and they lower the density by breaking up the tetrahedral Si–O bonding. However, the carbon component is susceptibleto degradation when exposed to the reactive plasmas used for capping, etching, and ashing processes, especially oxidizing plasmas that induce silanol formation. Such plasma-induced chemical modifications can cause film densification, dangling bonds and defects, and moisture uptake.[5,6]

Recently, International SEMATECH monitored several OSG films for change in κ caused by integration damage (ID) while integrating the films into SEMATECH's Cu/Damascene test chip using their standard processing flow (Table I).[7]

Mesoporous OSG films with connected pores exhibited a large increase in κ due to ID during integration. In contrast, nonmesoporous OSG films showed much smaller changes in κ. Thus, connected mesoporosity appears to facilitate film damage during processing by allowing reactive species to more easily penetrate the film.

Various plasma pretreatments (PPT) have been reported to form densified and chemically modified interface layers on OSG films, and these skin layers can prevent film damage by photoresist ash processes.[8–10] This study reports the effects of oxygen and nitrogen-based plasmas on one mesoporous and two nonmesoporous blanket films. To our knowledge, this is the first direct demonstration that a mesoporous film is more susceptible to ID than its nonmesoporous counterpart.

OSG-1 is a proprietary spin-on mesoporous methylsilsesquioxane (MSQ)-based film where porosity is created by thermal decomposition of a porogen that is incorporated into the MSQ-based film. The mesoporosity of OSG-1 is about 58%. Positronium annihilation lifetime spectroscopy (PALS)[11] determined that the average pore diameter is 2.5 nm and that the pores are 80–100% connected to the surface of the film. OSG-1 was deposited using a TEL Mark-8 spin-coater and oven-cured at 425 °C. OSG-2 is the nonmesoporous version of OSG-1 deposited with the same MSQ-based precursor but without the porogen. OSG-2 was spin-deposited and cured for less time at 450 °C by the supplier. The MSQ-based precursor for both OSG-1 and OSG-2 contains approximately 12% carbon.[12] OSG-3 is a trimethylsilane-based, plasma-enhanced chemical vapor deposited (PECVD)

[a)] Address all correspondence to this author.
e-mail: r6758c@email.sps.mot.com

 © 2001 Materials Research Society

TABLE I. SEMATECH data for several OSG low k films integrated into their standard test chip. The as-deposited κ-value increases by Δκ after integration due to ID. The κ after integration was extracted from capacitance measurements on interdigitated comb/serpentine structures using RAPHAEL™ simulation software.

Material	κ after integration	MOSCAP (blanket film)	Δκ
OSG-A	2.92 ± 0.11	2.92 ± 0.02	0
OSG-B	3.0 ± 0.30	3.07 ± 0.03	0.07
OSG-C	2.75 ± 0.30	2.76 ± 0.03	0.01
OSG-1	2.77 ± 0.12	2.2 ± 0.01	0.57
OSG-D	2.39 ± 0.10	2.09 ± 0.03	0.3
OSG-E	2.75 ± 0.30	2.12 ± 0.03	0.63
OSG-F	2.95 ± 0.30	2.29 ± 0.03	0.66

[a]OSGs A, B, and C are nonmesoporous PECVD films.
[b]OSGs 1, D, E, and F are mesoporous spin-on films with connected pores.

OSG film that also incorporates Si–CH_3 groups and contains approximately 18% carbon.[13] OSG-3 was not annealed after deposition.

The PPTs were conducted in a commercial PECVD tool at 350 °C (setpoint). A Gasonics (IPC L3500) asher was used for the oxygen plasma ashing. Thickness and refractive index (RI) were measured with a Woollam variable-angle spectroscopic ellipsometer (VASE). Standard Hg-probe MIS metal-insulator-semiconductor MOS capacitor (MOSCAP) measurements determined the κ-value, and Fourier transform infrared (FTIR; BioRad QMS-408M) spectra were collected in transmission mode. Cross-sectional scanning electron microscope (XSEM) samples were stained by a 2 s buffered oxide etch (BOE) dip to highlight modified layers in the films prior to imaging in a Hitachi 5000H with a low beam current to prevent damage to the low κ films.

The XSEM images in Fig. 1 and time-of-flight secondary ion mess spectrometry (TOF-SIMS) (not shown) show that the PPT causes a thin (<100 Å) skin layer to form on the nonmesoporous OSG-2 that protects it from subsequent ash damage. Ashing OSG-2 without a PPT caused a very thick densification layer. OSG-3 exhibited nearly identical behavior. The PPT modified layer is limited to the surface for the exposure times used because its growth rate is very slow. In contrast to the nonmesoporous OSG films where the skin layer remains very thin at the film surface, XSEM images of OSG-1 after PPTs for 30 and 60 s (Fig. 2) show a densification layer that grows thicker with PPT time. TOF-SIMS depth-profiled chemical analysis[7] determined that the densification layer is nitridated by the PPT for all three films consistent with previous findings on similar OSG films.[8,10] Some fluorination is also observed due to residual fluorine in the plasma chamber. The nitrided layer also grew deeper with increasing PPT time. TOF-SIMS indicates that ashing caused only densification without nitridation.

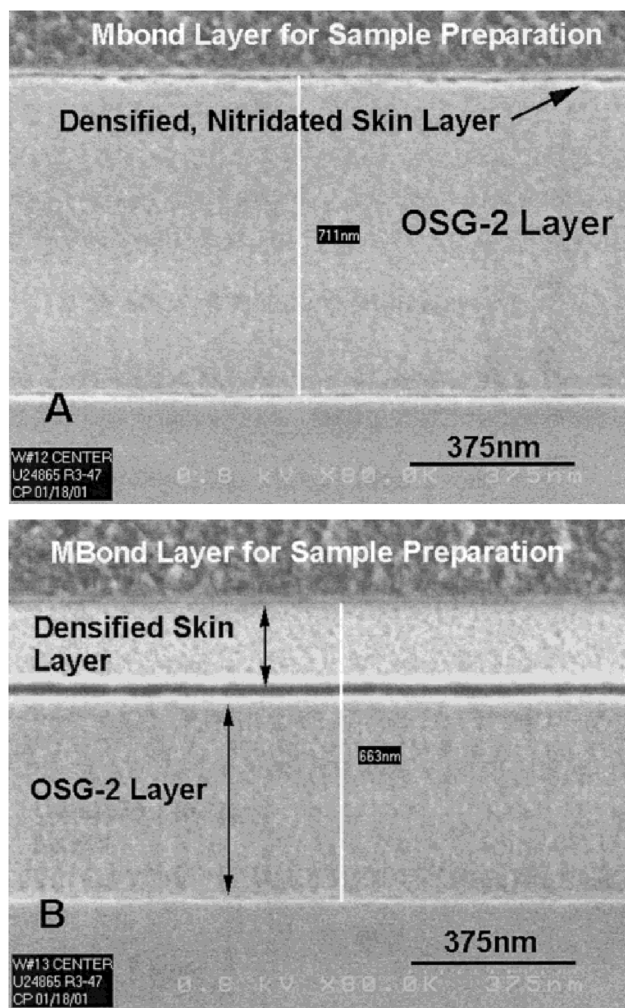

FIG. 1. XSEM images of OSG-2: (A) 60 s PPT (N-based) only, and (B) 10 s O_2 plasma ash only. A 60 s PPT + 10 s O_2 plasma ash looked identical to image A. An MBond layer was deposited on top of the OSG-2 film to facilitate sample preparation.

Figures 3–5 show how κ, Si–CH_3 absorptions, and RI change after a 60 s PPT, 60 s PPT + 10 s O_2 plasma ashing, and after ashing without a PPT.

The aforementioned properties are relatively constant for the nonmesoporous OSG films after both the 60 s PPT and 60 s PPT + ash. However, without the PPT, ashing causes substantial changes in these properties. Thus, the 60 s PPT effectively protects OSG-2 and OSG-3 from ash damage by stabilizing the films' properties.

In contrast to the nonmesoporous films, the 60 s PPT does not protect the mesoporous OSG-1 from ash damage, and the PPT alone causes large changes in the film's properties. The thickness decreases and RI increases, the κ-value increases above 4.0, and the Si–CH_3 peaks completely disappear. The κ value increases because of densification, silanol formation, and water absorption. Silanol and water absorptions increase in the FTIR (not shown) as the Si–CH_3 peaks decrease.

Figure 6 shows that the percent $–CH_3$ in OSG-1 changes continuously with PPT time. As the PPT time increases, the $–CH_3$ absorption decreases. The RI also increases and the thickness decreases with PPT time (not shown). Although lowering the PPT time lessened the severity of damage to OSG-1, even the 15 s PPT substantially damaged OSG-1 and did nothing to protect the film from subsequent ash damage.

These results demonstrate that the mesoporous OSG-1 is much more susceptible to ID than are the nonmesoporous OSG films. In the cases of OSG-2 and OSG-3, the PPT forms a skin layer that effectively barriers the rest of the film from damage during ashing, at least for the plasma exposure times used in this study. A skin layer also forms on the surface of OSG-1, but this layer does not seal off the rest of the film from the reactive species in the PPT or ash plasmas. Although only two plasmas (oxygen- and nitrogen-based) were used in this study, the data suggest that the mesopores are more difficult to

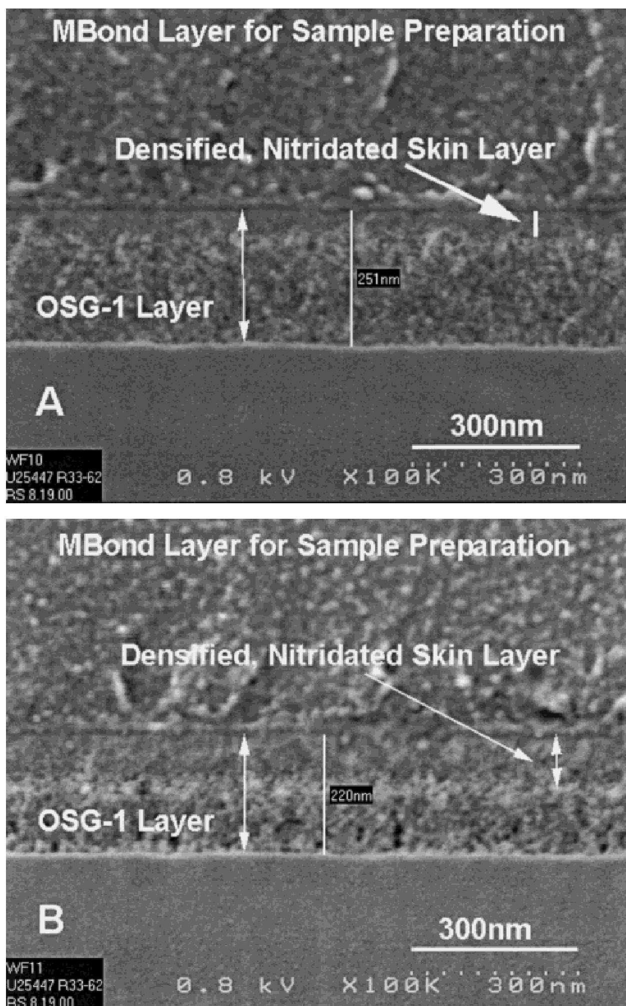

FIG. 2. XSEM images of OSG-1: (A) 30 s PPT (N-based) only, and (B) 60 s PPT (N-based) only. An MBond layer was deposited on top of the OSG-1 film to facilitate sample preparation.

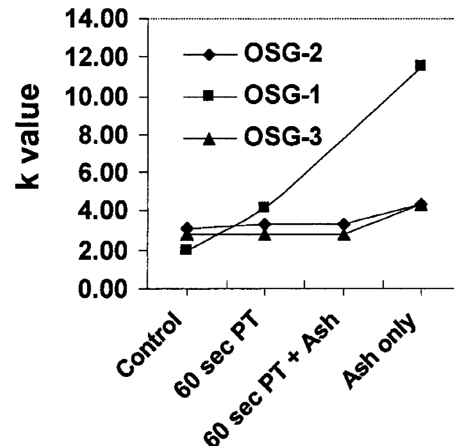

FIG. 3. Hg-probe MIS MOSCAP data showing κ versus condition.

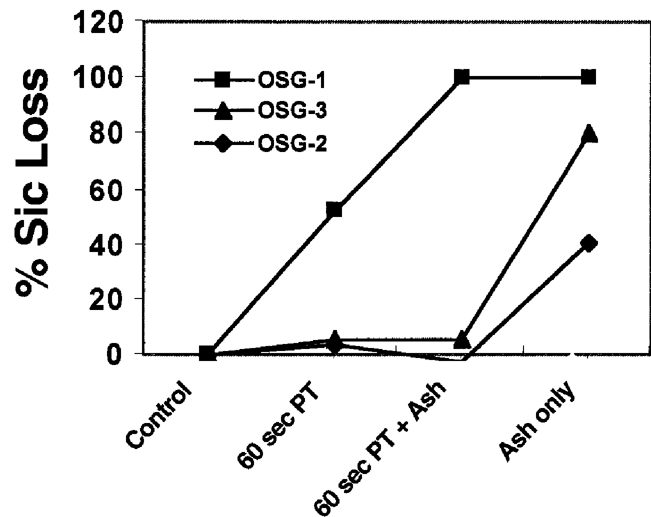

FIG. 4. The percent loss of the $Si–CH_3$ peak (approximately 1275 cm^{-1}) area versus process condition. The data is normalized for thickness variations. The $–CH_3$ peak at approximately 2970 cm^{-1} shows a similar trend.

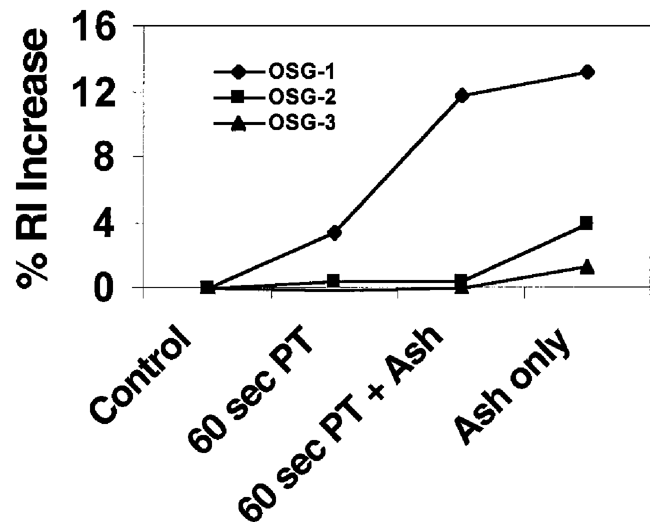

FIG. 5. The percent change in RI (at 630 nm) versus process condition.

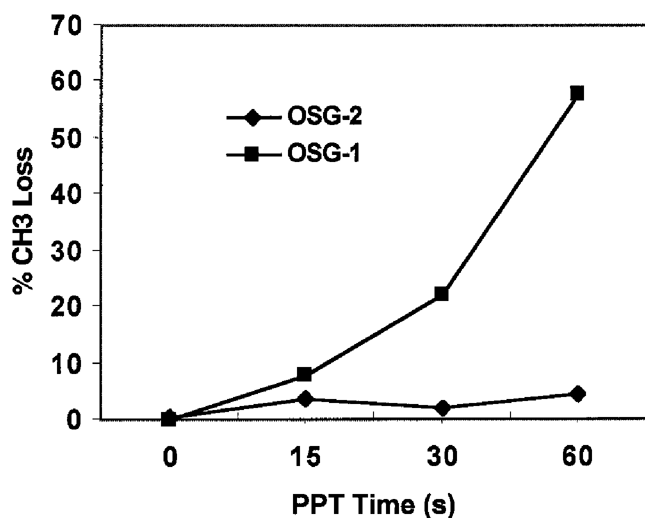

FIG. 6. The percent loss of the $–CH_3$ FTIR peak (approximately 2970 cm^{-1}) area versus PPT time. The data is normalized for thickness variation. The Si–C peak at approximately 1275 cm^{-1} shows a similar trend.

close off at the surface of the film, and the connected pore structure allows reactive species in plasmas to more rapidly penetrate the film beyond the densified interface layer. However, lower density alone may be responsible. The results also suggest that films with isolated pores may be less susceptible to ID, but a closed pore OSG film was not available for this study. We are now exploring other plasma chemistries to determine if they are more benign to mesoporous OSG films, and we are using PALS to explore the effect of pore size and pore structure on the diffusion of reactive species that cause ID.

In summary, a mesoporous OSG film was found to be more susceptible to ID than its nonmesoporous counterpart and a nonmesoporous PECVD OSG film. A nitrogen-based plasma forms a dense, nitridated skin layer on the nonmesoporous OSG films, which protects them from subsequent plasma damage. The skin layer was not confined to the surface of the mesoporous OSG and grew deeper into the film with exposure time. The results suggest that the connected pore structure provides easy diffusion paths for reactive species.

ACKNOWLEDGMENTS

We gratefully acknowledge the staff at Motorola's Dan Noble Center and International SEMATECH who contributed to various aspects of this work.

REFERENCES

1. W.W. Lee and P.S. Ho, MRS Bulletin **22** (10), 19 (1997).
2. M. Morgen, E.T. Ryan, J-H. Zhao, C. Hu, T. Cho, and P.S. Ho, Ann. Rev. Mater. Sci. **30,** 645 (2000).
3. E.T. Ryan, H-M. Ho, W-L. Wu, P.S. Ho, D.W. Gidley, and J. Drage, IITC Proc. 187 (1999).
4. E.T. Ryan, S. Lin, D. Nelsen, J. Wetzel, D. Gidley, and J. Drage, Adv. Metal. Conf. Proc. (2000, in press).
5. E. Kondoh, M.R. Baklanov, H. Bender, and K. Maex, Electrochem. Solid-State Lett. **1,** 224 (1998).
6. R.K. Iler, *The Chemistry of Silica* (Wiley, New York, 1979).
7. E.T. Ryan, S. Lin, and J. Wetzel (unpublished).
8. T.C. Chang, P.T. Liu, Y.S. Mor, S.M. Sze, Y.L. Yang, M.S. Feng, F.M. Pan, B.T. Dai, and C.Y. Chang, J. Electrochem. Soc. **146,** 3802 (1999).
9. P.T. Liu, T.C. Chang, Y.S. Mor, and S.M. Sze, Jpn. J. Appl. Phys. **38,** 3482 (1999).
10. P.T. Liu, T.C. Chang, Y.L. Yang, Y.F. Cheng, and S.M. Sze, IEEE Trans. Elect. Dev. **47,** 1733 (2000).
11. D.W. Gidley, W.E. Frieze, T.L. Dull, A.F. Yee, H.M. Ho, and E.T. Ryan, Phys. Rev. B **60,** R5157 (1999).
12. Data provided by the material supplier.
13. Unpublished SEMATECH data.